

# The 2018 EXPORTS Pacific Experiment

## Calibration of Oxygen Sensors on Lagrangian Float #92

Eric A. D'Asaro

Applied Physics Laboratory, University of Washington

Version 2.0 Nov. 18, 2019

### Summary

EXPORTS Lagrangian float (#92) carried two optode oxygen sensors, a Seabird SBE-63 and a Xylem Aanderaa 4330, measuring at the same level as the CTD. These were primarily calibrated using Winkler measurements on bottle samples from the *R/V Sally Ride* and *CCGS Tully* with additional calibrations provided by measurements of oxygen concentrations in the air by the same sensors during float surfacings, and by the pre-cruise and post-cruise manufacturer calibrations. Special analyses were necessary to compensate the air measurements for the frequent immersions of the sensor. The final calibration was very close to the post-cruise calibrations and expressed as 1.034 times the pre-cruise calibration value and accurate to  $\pm 2 \mu\text{mol kg}^{-1}$ . However, this accuracy only applies to data within the mixed layer and to data taken during the isopycnal drifts of the float at the  $25.85 \text{ kg m}^{-3}$  isopycnal. During the profiles transiting between these levels, both sensors show anomalous values of approximately  $\pm 20 \mu\text{mol kg}^{-1}$  due to their slow response in both temperature and oxygen. A small number of Seabird measurements are also anomalous, apparently due to temporary clogging of the flow path. These artifacts are not corrected in this data release. Data is released in two files one for the Aanderaa and one for the Seabird. The Aanderaa data is the preferred measurement due to the higher sampling rate and lack of the pump anomalies. The data from the two sensors is otherwise of similar accuracy.

### 1. Sensors & Mission

Float 92 (Fig 1) was the only Lagrangian float deployed in EXPORTS 2018. It carried SBE-41-CT sensors on the top and bottom endcaps with the entrances to the pumped sensors separated vertically by 1.7 m.

Oxygen was measured by two sensors, an Aanderaa 4330 (SN 1222) mounted at the same level as the top CTD intake (see Fig. 1) and a Seabird SBE63 (SN 1826) plumbed in line with the pumped CTD sensors. Thus, both sensors measure almost the same water. The temperature and salinity measured by the top CTD is assigned to oxygen measurements at the same time. Both sensors measure water temperature and the fluorescence lifetime of the same PreSens PSt3 material. Quenching of this fluorescence by oxygen provides a

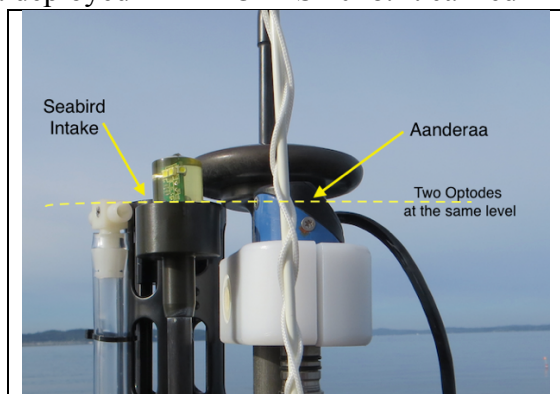


Fig. 1. Aanderaa oxygen sensor (blue) mounted on top of float 92 at the same level as the top CTD intake. Seabird oxygen sensor is plumbed into the CTD and samples the same water as the temperature and conductivity sensors.

measurement of oxygen partial pressure, which is converted to oxygen concentration. Both sensors were calibrated before (AA: Jan 26 2018; SBE: Jan 3 2018) and after (AA: Sep 19 2019; SBE: July 27 2019) the deployment. Realtime data used the pre-cruise calibrations. The analysis here uses the pre-cruise calibrations, although the post-cruise calibrations are found to be much closer the final calibrated values.

Float 92 was deployed on 14-Aug-2018 07:15Z from the *R/V Sally Ride*, sampled for 109.3 days with the last data taken on 01-Dec-2018 14:34 Z. The float was recovered shortly thereafter by *R/V Sikuliaq*. The Aanderaa optode sampled 101198 data points, with an average separation of 98 seconds. The Seabird optode sampled 14106 points with an average separation of 664 seconds. The float also successfully measured temperature, salinity, pressure, nitrate, optical backscatter and chlorophyll fluorescence. The accuracy of these sensors is described in other data reports.

Calibration casts were made from the *R/V Sally Ride* during the main experimental period, from the *CCGS Tully*, in late September and from the *R/V Sikuliaq* at recovery. The minimum separation between the cast and the float was less than a kilometer at the same time, except for the *R/V Sikuliaq* cast which occurred at the same location as the float, but a day earlier.

The float executed a simple mission (Fig. 2) alternating between daily profiles to 200 m and a Lagrangian drift at approximately 100 m. More precisely, during the drift the float targeted the  $25.85 \text{ kg m}^{-3}$  isopycnal maintaining this isopycnal between the top and bottom CTDs as it moved vertically  $\pm 10\text{m}$  due to internal waves and tides and mesoscale eddies (Fig. 3). Profiles occurred once per day, timed to approximating 0130Z during the cruises so as to facilitate calibration casts, and to approximately 1300Z thereafter, so as to facilitate nighttime air calibrations of the oxygen probe.

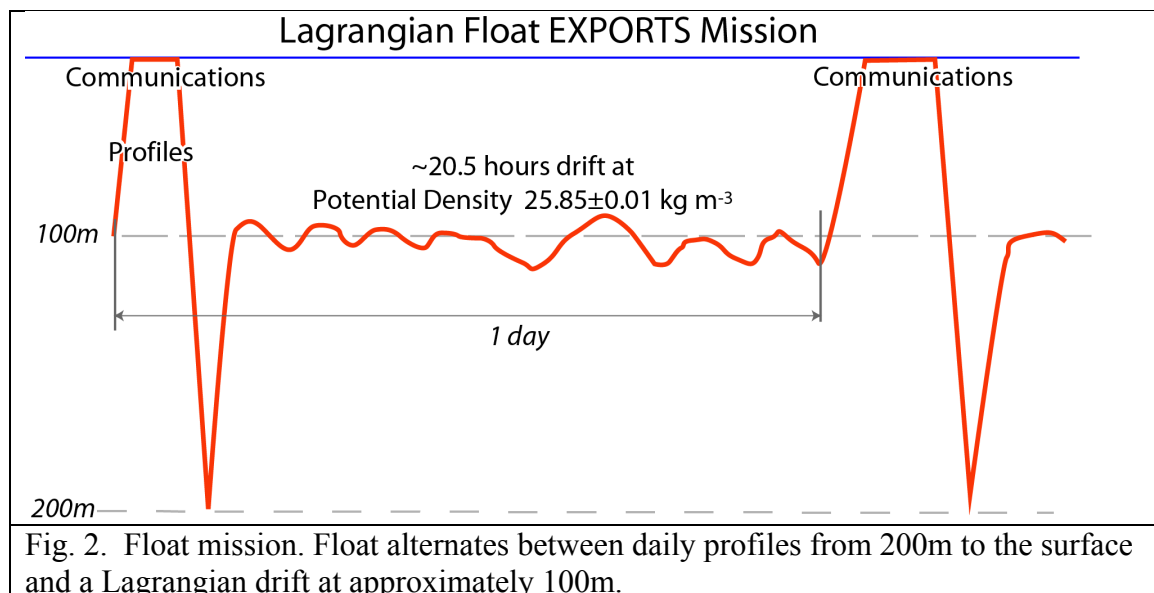


Fig. 2. Float mission. Float alternates between daily profiles from 200m to the surface and a Lagrangian drift at approximately 100m.

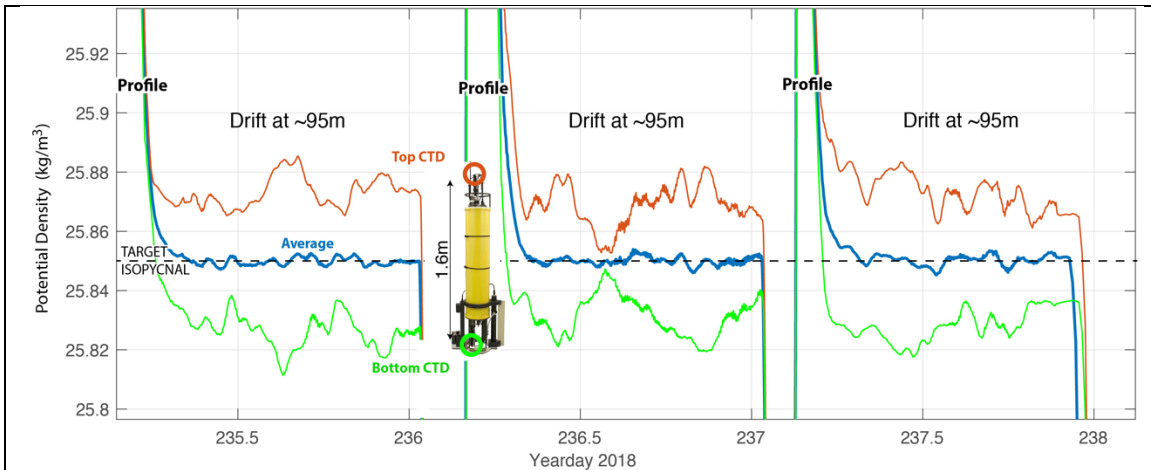


Fig. 3. Example of isopycnal drift. Float straddles target isopycnal with an accuracy of about 0.1 m.

The Aanderaa optode was sampled every 100s during the drift and 15-75s during profiles depending on other activities. The Seabird optode was sampled by a factor of 11 less during the drifts and of 3 less during the profiles.

## 2. Ship CTD calibration

The float oxygen sensors were primarily calibrated using the Winkler bottle sample from the *R/V Sally Ride* taken in the mixed layer. However, these samples had duplicate variations of several  $\mu\text{mol/kg}$  which make direct comparisons with the float data difficult. It was thus better to use the bottle samples to calibrate the SBE-43 oxygen sensor on the *R/V Sally Ride* CTD and then calibrate the float sensors against the CTD sensor.

Analysis was done on data from the *R/V Sally Ride* bottle file *SallyRideSIOBottleFiles\_v3.csv*. The first two bottle casts were discarded as they have high noise and an offset relative to later casts. A few points with differences larger than 10  $\mu\text{mol/kg}$  were also discarded. Figure 4 shows a scatter plot of the CTD and bottle samples. The deep values show little spread and thus yield an accurate estimate of the CTD offset at zero oxygen, -2.26  $\mu\text{mol/kg}$ . However, the shallower values have a large spread, so it is not obvious that a least squares line gives the best value. Figure 5 limits the analysis to only the mixed layer (Pressure < 20 dbar, magenta points) thus avoiding the regions of very large oxygen

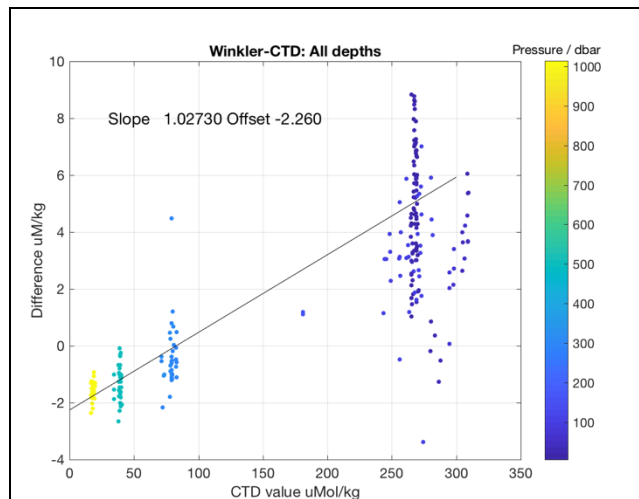


Fig. 4. Scatter plot of uncalibrated SBE43 and Winkler bottle samples colored by pressure. The final calibration line is shown.

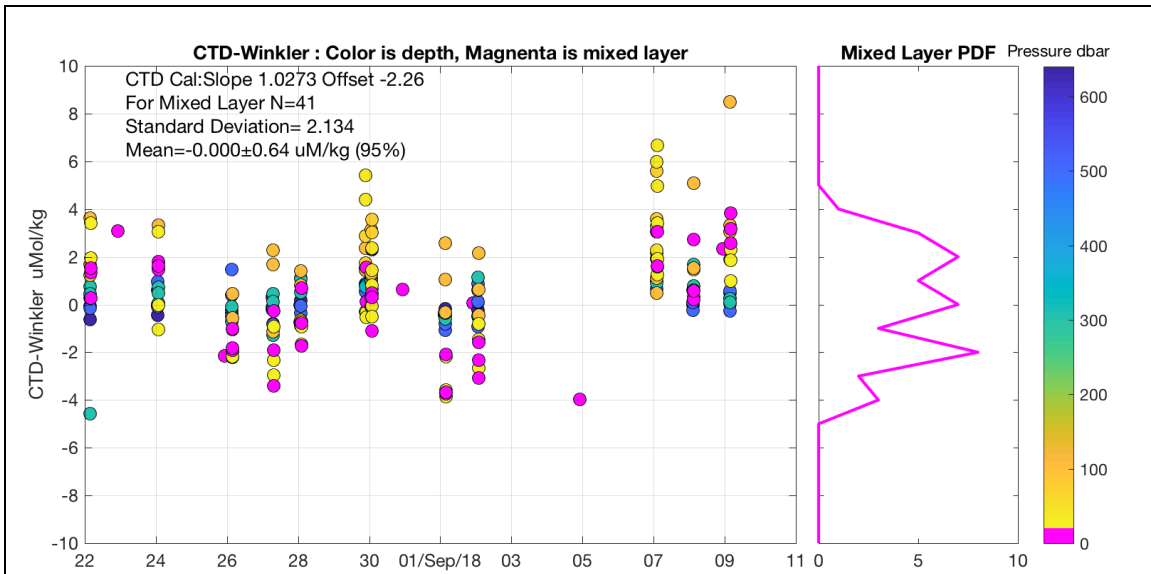


Fig. 5. Difference between calibrated SBE43 oxygen and bottle samples colored by pressure. Mixed layer values are magenta. PDF of mixed layer values is shown on the right. Offset of calibration is chosen from Figure. 4. Slope of calibration is adjusted to yield zero mean for mixed layer values.

gradient where errors are likely to be larger. There are no clear trends in either depth or time. The calibration slope is adjusted to yield zero mean difference between the bottles and CTD in the mixed layer. The standard deviation of the Winkler values is about 2  $\mu\text{mol/kg}$  and is close to Gaussian. Averaging over all 41 values yields a 95% error in the mean of 0.64  $\mu\text{mol/kg}$ , with similar values for a bootstrap or Gaussian analysis.

The CTD values have thus been adjusted by

$$[\text{O}_2]_{\text{calibrated}} = 1.0273 [\text{O}_2]_{\text{v3file}} - 2.26 \mu\text{mol/kg}$$

### 3. Time Response

Figure 6 shows a typical profile of oxygen from both sensors. From the isopycnal drift, the float profiles up to the surface, then down to 180 dbar, and then back up to the isopycnal. The profiling is imperfect, with large variations in the profiling speed. The Aanderaa samples more rapidly than the Seabird.

For both sensors, the depth of the maximum in oxygen at about 50 m is displaced upward on the up profile and downward on the down profile, indicating a lag in the sensor response. However, the measured oxygen is larger on the down profile than on the up profile, both above and below the maximum. This cannot be explained by a sensor lag alone. Instead, it is likely due to the dependence of the measured oxygen on temperature (higher temperature leads to a lower oxygen measurement) and a mismatch between the time response of the temperature and fluorescence parts of the measurement. A detailed analysis is beyond the scope of this report and this effect will not be removed from this release of the data.

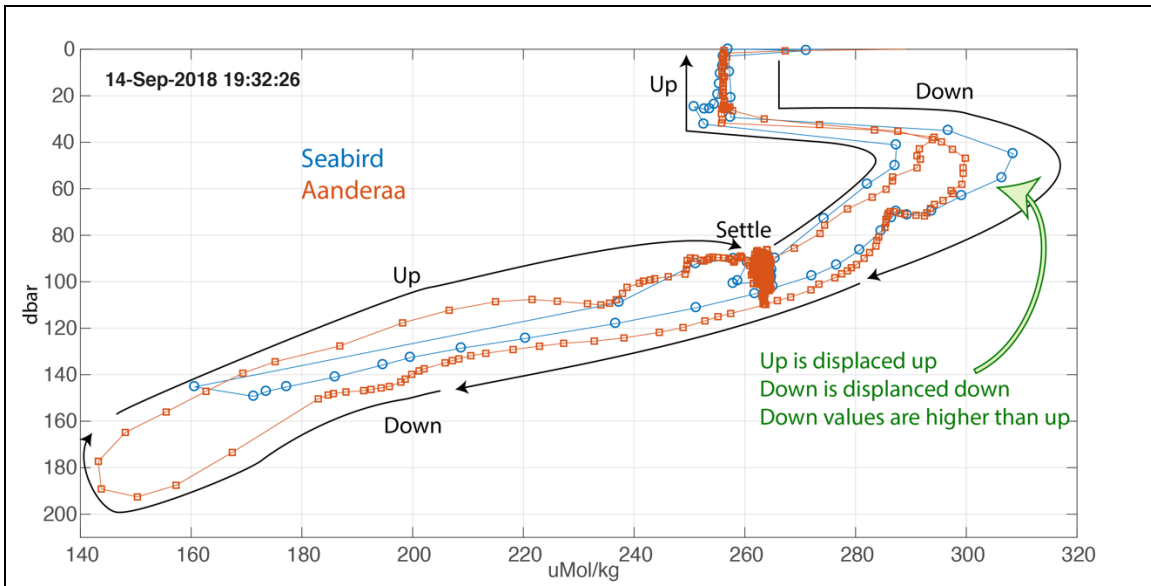


Fig. 6. Typical profile of oxygen from both sensors. Blue lines are SBE-63; red lines are Aanderaa. Symbols mark data samples. Black lines show sense of motion.

#### 4. Aanderaa v. Seabird time series

Without correcting for these large time response profiles, the sensors can only be calibrated and compared in the mixed layer and during the drifts. Figure 7a shows timeseries of both sensors in the mixed layer, defined as pressures between 15 and 0.5 dbar and salinities greater than 31 psu. This latter criterion is necessary to exclude data points when the float is at the surface and the top CTD is out of the water. Figure 7d shows time series of both sensors during the isopycnal drifts, defined as potential density between 25.81 and 25.87  $\text{kg m}^{-3}$  and vertical speed less than 5 cm/s. This latter criterion is necessary to exclude data points within this isopycnal range during profiles.

The two sensors track very closely except for a few times in early September when the Seabird sensor reads low. This appears to be due to clogging of the pumped plumbing. Figures 7b and 7d plot the difference between the two sensors (black) and running means

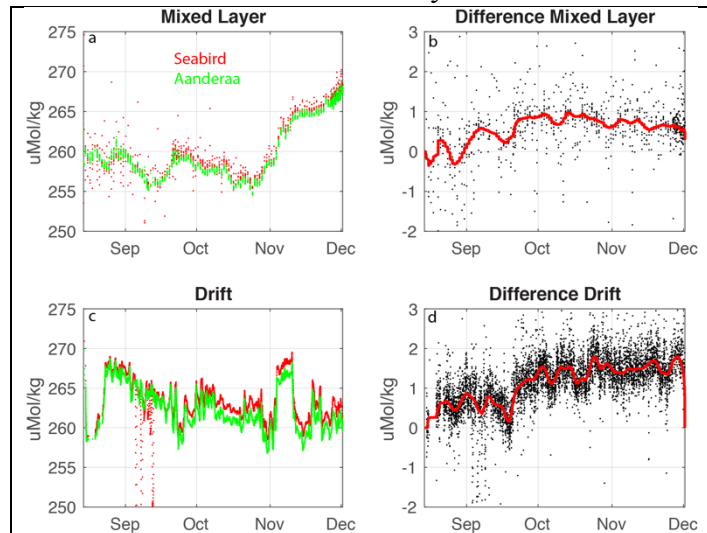


Fig. 7. Time series of oxygen in the a) mixed layer and c) isopycnal drift for the Seabird (red) and Aanderaa (green) optodes. Seabird-Aanderaa values (black) are plotted in b) mixed layer and d) isopycnal drift with averaged values (red)

(red) of the differences (31 points for the Seabird and 251 points for the Aanderaa). On average, the Seabird reads about 1  $\mu\text{mol/kg}$  higher than the Aanderaa. There is a small ( $\sim 0.7$   $\mu\text{mol/kg}$ ) increase in the difference on September 10. Whether this change occurs in the Seabird or Aanderaa sensor could not be determined.

Thus, except for the bad points and this small calibration difference, the two sensors behave very similarly. Since the Aanderaa is sampled more frequently it is the preferred sensor for further analysis.

### 3. Air Calibrations

Secondary oxygen calibrations were made by measuring the partial pressure of oxygen in the atmosphere during float surfacings. Due to differences in the float behavior and configuration, these methods differ in some details from those described by Bittig et al. (2016, 2018), Bushinsky et al. (2016) and Johnson et al. (2015).

Ocean surface temperature (SST) and salinity (SSS) were obtained from the daily float mixed layer values. Atmospheric surface layer variables at height  $Z_{ERA}=2\text{m}$  at the float location were obtained by interpolating the ERA5 (NCAR RDA dataset ds633.0 “ERA5 Reanalysis” – October 2019) to the float location. Comparison with measurements at nearby Ocean Weather Station P found surface pressure ( $P_{atmos}$ ) differences always less than 1 hectopascal, air friction velocity ( $u_*$ ) differences always less than 0.1 m/s, and 2 m relative humidity ( $RH$ ) and air temperature ( $T_{air}$ ) from ERA5 biased low by about 55 and 0.25 C respectively. Difference between OWSP and the float from ERA5 become many times larger toward the end of the record. ERA5 values were thus used at the float with the uncertainties estimated from the OWSP differences.

The partial pressure of oxygen in air at the height of the float sensors during air calibration ( $Z_{fl}=0.26\text{m}$ ) was computed as

$$pO_{2air} = \chi_{O_2} (P_{atmos} - P_{H_2O}) \quad (1)$$

where  $\chi_{O_2} = 0.20946$  is the fractional concentration of  $O_2$  in the atmosphere and  $P_{vapor}$  is the vapor pressure at  $Z_{fl}$  computed as

$$P_{vapor} = P_{vap0}(SST, SSS) + (RH P_{vap2} - P_{vap0}) \log\left(\frac{Z_{fl}}{Z_0}\right) / \log\left(\frac{Z_{ERA}}{Z_0}\right) \quad (2)$$

where  $P_{vap2}(T_{air}, P_{atmos})$  is the saturation vapor pressure at 2m and  $P_{vap0}(SST, SSS)$  is the saturation vapor pressure above seawater. Several different functions are used to compute saturation vapor pressure. The most general is Naya et al (2016) also available at [http://web.mit.edu/seawater/2017\\_MIT\\_Seawater\\_Property\\_Tables\\_r2a.pdf](http://web.mit.edu/seawater/2017_MIT_Seawater_Property_Tables_r2a.pdf).

Difference between this and the equation used by Aanderaa is about 0.2% for fresh water at atmospheric pressure. Salinity changes the vapor pressure by about 2%.

The natural log terms translate the ERA5 data at  $Z_{ERA}=2\text{m}$  to the float sensors at  $Z_f=0.26\text{ m}$  assuming a neutrally stratified atmospheric boundary layer and a roughness length computed from the Charnock relation  $Z_0=0.015 u_*^2/g$ , where  $g=9.8\text{ m}^2/\text{s}$ .

The partial pressure of oxygen in water was computed as described in the Aanderaa manual. The sensor outputs a partial percent saturation  $psat_{AA}$  which is converted to partial pressure by

$$pO_{2water} = \frac{psat_{AA}}{100} (P_{atmos0} - P_{vap}(T_{optode})) \chi_{O_2} \quad (3)$$

where  $P_{atmos0} = 101325\text{ Pa}$  is standard atmospheric pressure.

The height of the optode above the surface during air calibrations was computed using subsurface pressure measurements on the float. Atmospheric pressure during the measurements varied by  $\pm 0.2\text{ dbar}$ , more than the height of the optode above the surface. Accurate measurements of the height, thus must be compensated for atmospheric pressure.  $P_{atmos}$  was subtracted from the measured float pressure to reference it to the surface. Unlike ARGO floats, the Lagrangian floats continue to operate the top CTD as the float reaches the surface. As shown in Fig. 7, as the CTD comes out of the water, the conductivity sensor fills with air and the salinity measurement drops to nearly 0. The transition is 0.2-0.4 m wide. The ‘surface pressure’ is chosen as the depth where the average salinity is about half the surface value, as shown in Fig. 7 and pressure is referenced to this value.

A similar transition occurs for the  $pO_2$  measurement by the optode as sketched in Fig. 8. Below the surface, the optode measures  $pO_{2water}$ . As it reaches the surface, it will measure a mixture of  $pO_{2air}$  and  $pO_{2water}$ , with the mixture depending on the behavior of the float at the surface and the sea state. If the float

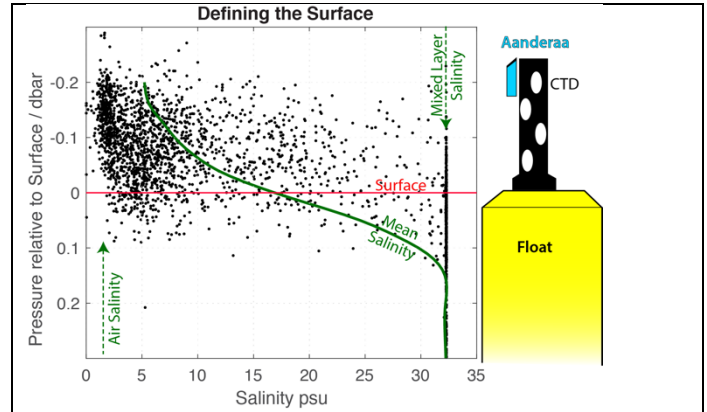


Fig. 7. Profiles of salinity as a function of pressure as the float reaches the surface. A sketch of the float is shown to scale. The effect of atmospheric pressure variations has been removed. All salinity values from the top CTD near the surface are plotted. Green lines show measured salinities in mixed layer, and in the air (dashed) and the average measured value (solid).

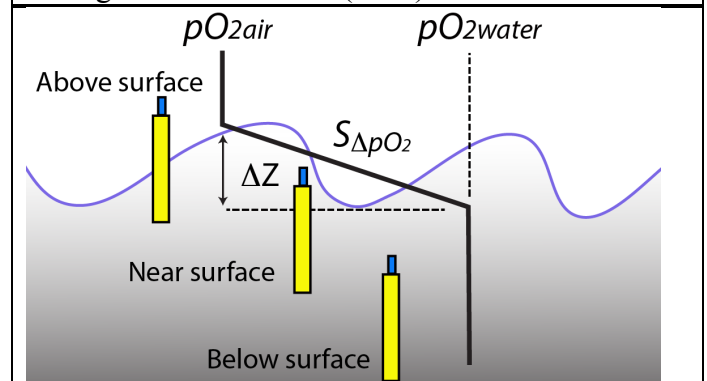


Fig. 8. Partial pressure measured by the optode varies from  $pO_{2water}$ , when the float is below the surface, to  $pO_{2air}$ , when it is sufficiently above the surface. The thickness  $\Delta Z$  of the transition region depends on the behavior of the float and the sea state.

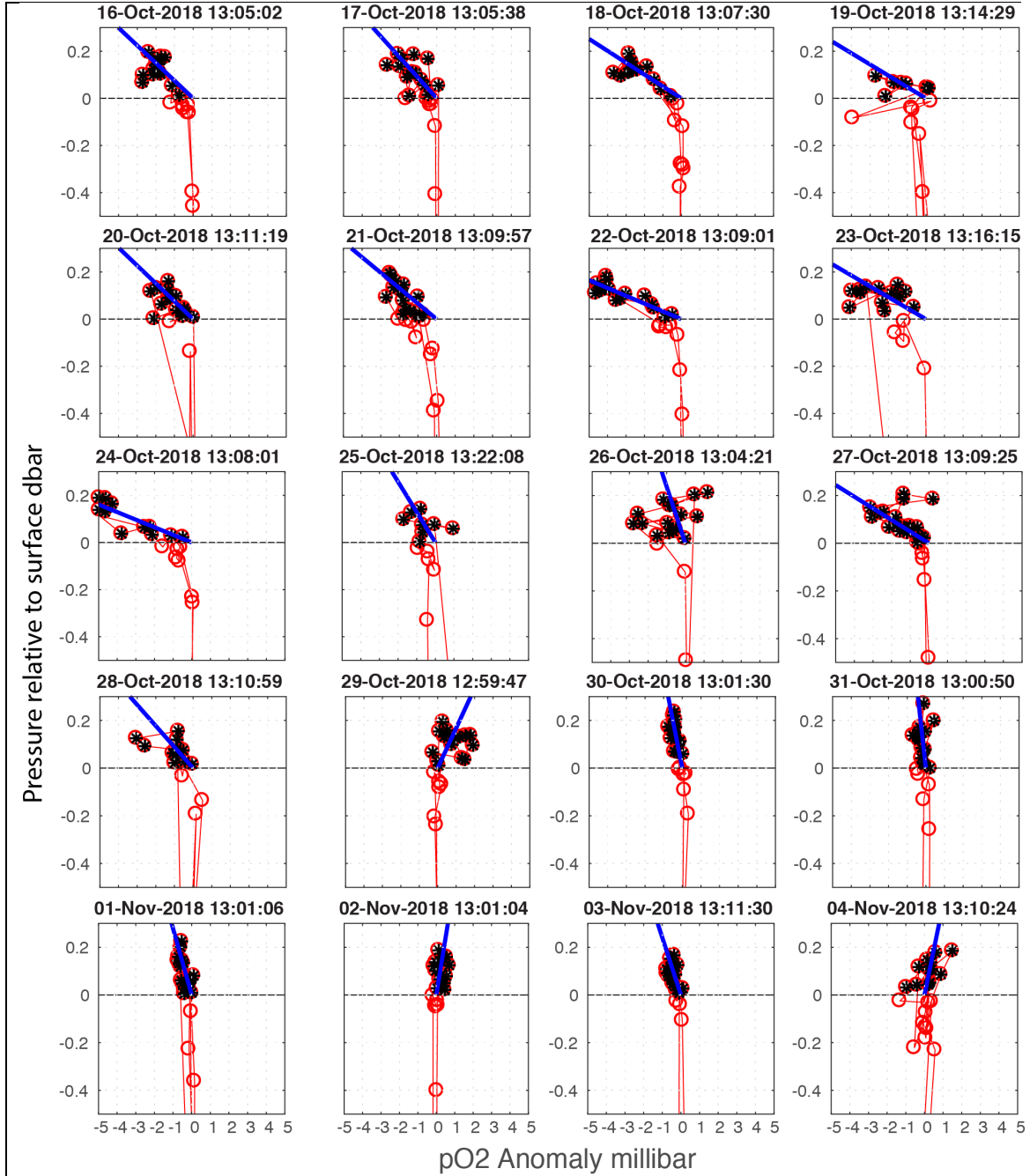


Figure 9. Daily profiles of  $pO_2$  relative to the mixed layer for 20 days during which the air-sea difference in  $pO_2$  changes sign. Format is similar to Fig. 7, but for the profile of  $pO_2$  instead of salinity. The blue line shows the slope  $pO_2$  across the interface.

is sufficiently buoyant and the optode sufficiently high, the optode will measure  $pO_{2air}$ . The transition layer thickness is  $\Delta Z$  and the average slope is  $S_{\Delta pO_2}$ . Thus,

$$\widetilde{pO_{2air}} = pO_{2water} + S_{\Delta pO_2} \Delta Z. \quad (4)$$

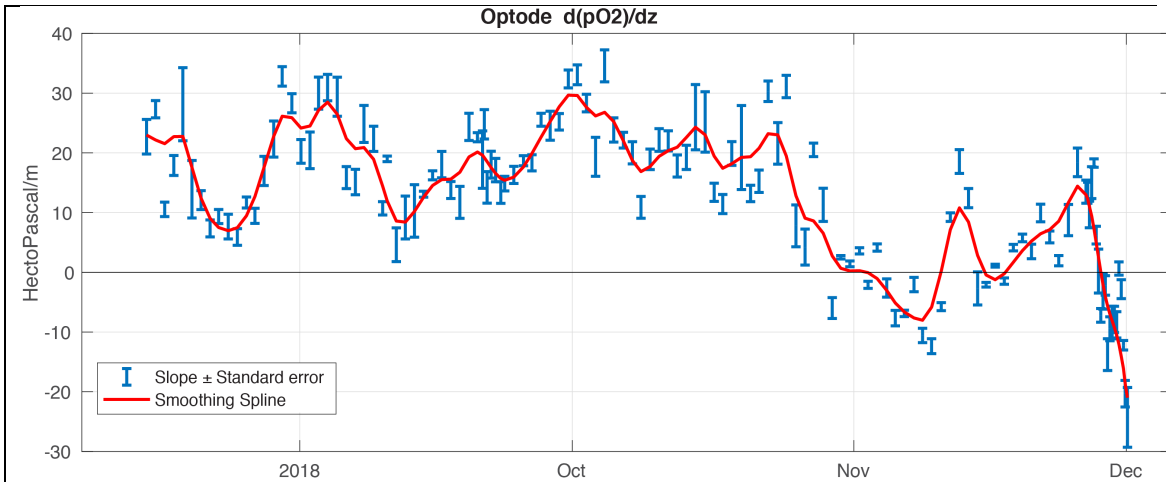


Fig. 10. Air-Sea slope in  $pO_2$  for all float surfacings. Red line is a smoothing spline fit through these points.

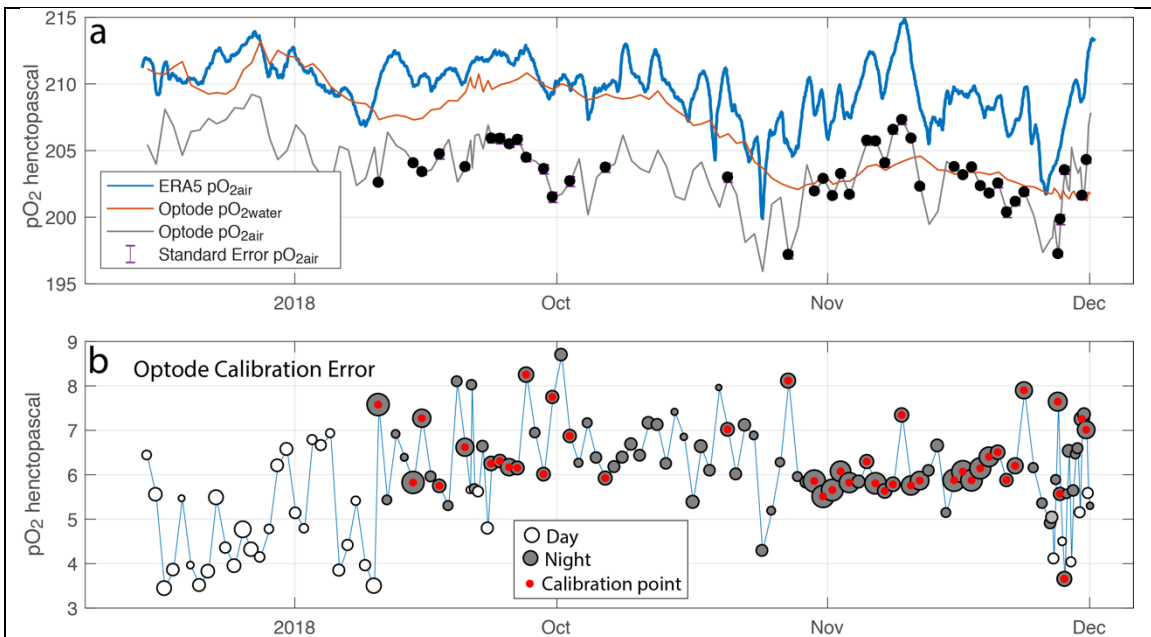


Fig. 11. a)  $pO_{2air}$  from ERA5 (blue),  $pO_{2water}$  from uncalibrated optode (red) and  $pO_{2air}$  from uncalibrated optode (gray) with chosen calibration points (black) and standard errors (mostly hidden). b) Calibration error  $\widehat{pO_{2air}} - pO_{2air}$ . White circles are from daytime; gray are from nighttime. Large circles have smaller errors than small circles. Red dots mark chosen calibration points.

where the tilde indicates that this is the value estimated by the float.

Compared to other Lagrangian floats, the EXPORTS float had too little drag and thus did not follow the surface well. Thus, as with ARGO floats, the optode remained within the transition region and never measured  $pO_{2air}$ . In the future, this can be improved by increasing the drag or making the optode to a higher location. From Fig. 7, it appears that

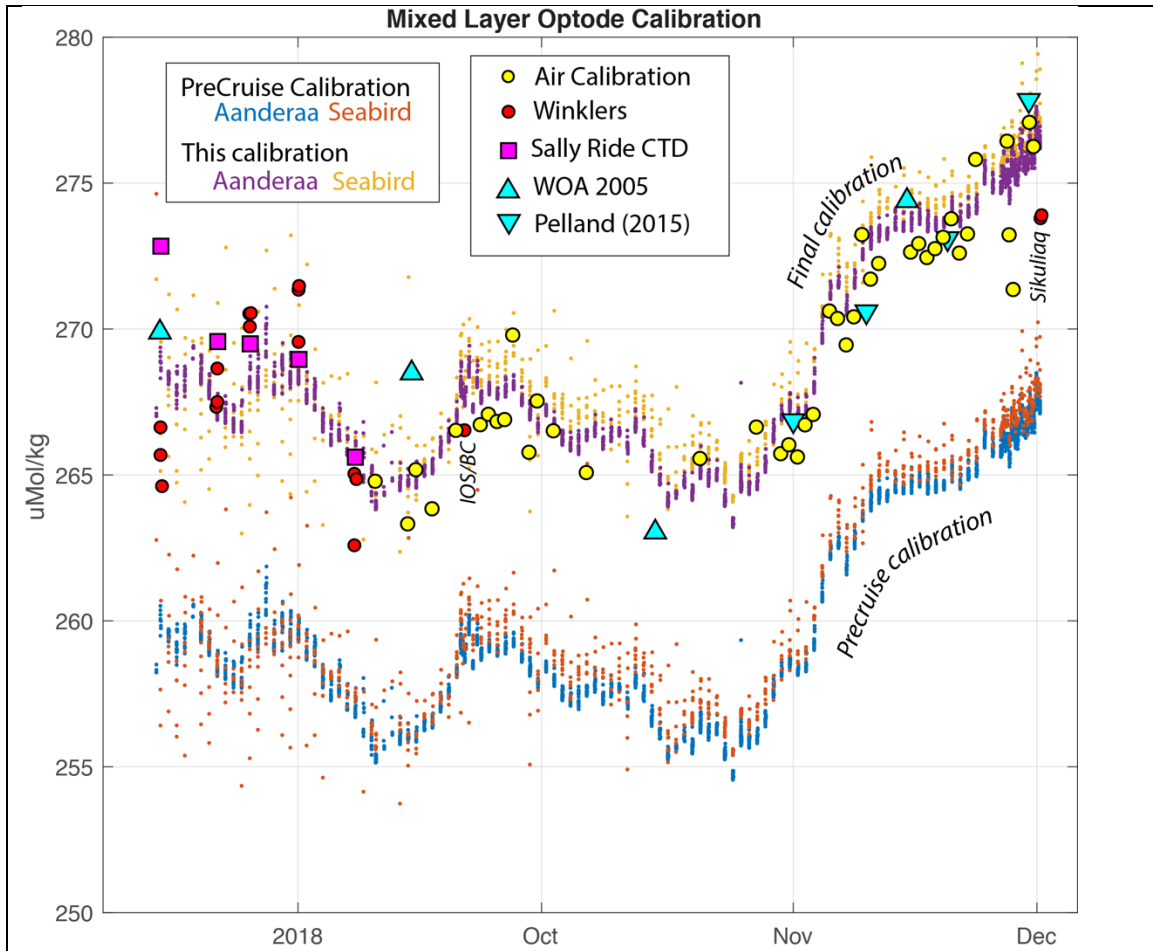


Figure 12. Optode calibration. All mixed layer optode estimates of oxygen concentration (dots) using pre-cruise calibrations (AA blue, SBE red) and final calibrations (AA purple, SBE orange) compared to multiple calibration points: Winkler bottle samples (red circles) and CTD data calibrated to Winklers (red boxes); air calibration points from Figure 11 (yellow circles) and historical data (cyan triangles) from NOAA World Ocean Atlas (Boyer et al. 2006) and data from Pelland (2015) indicating 99% saturation for November 2008 and 2009. The final Winkler value, labelled 'Sikuliaq' was taken a day before the float measurement and is thus not an accurate calibration.

moving the optode 0.1 to 0.2 m higher would greatly decrease the amount of water contamination. However, for this deployment, other approaches must be used.

The Lagrangian float measures its position relative to the surface and takes many measurements during each surfacing. It thus makes a profile through the near surface region on each surfacing. Figure 9 shows examples of these profiles, each fit with a line (blue) intersecting  $pO_{2water}$  at the surface. The slope of the line measures  $S_{\Delta pO_2}$ . In this example,  $S_{\Delta pO_2}$  is negative in the first panel (October 16),  $pO_2$  decreases away from the sea surface. By the last panel (October 31) the slope is nearly zero. This pattern can be seen in Figure 10 where the slope is positive in August, September and October, but goes through zero for the first time on about November 1.

The value of  $pO_{2air}$  is computed using (4) with,  $S_{ApO_2}$  computed from the float data (e.g. Fig. 10) and a fixed value of  $\Delta Z = 0.25\text{m}$ . The error in  $pO_{2air}$  is  $\Delta Z$  times the error in  $S_{ApO_2}$ . Figure 11a shows  $pO_{2air}$  ERA5 and from the optode  $\overline{pO_{2air}}$ . The difference, Figure 11b, is the calibration error. The calibration error is different for daytime calibration points (white circles) than for nighttime ones (gray circles). Calibration points for the optode were thus chosen to be only in the nighttime and to have errors in  $\overline{pO_{2air}}$  of less than 0.375 hectopascal.

## 4. Optode calibration

Figure 12 shows the final optode calibration compared to multiple calibration points. The realtime optode oxygen concentration using the precruise calibration (lower dots), is multiplied by 1.034 to form the calibrated optode data (upper dots). This value is very close to the ratio of postcruise to precruise Seabird calibrations, i.e. the final calibrations determined here is very close to the postcruise Seabird calibration. The calibrated optode data points are within  $\pm 2 \mu\text{mol/kg}$  of most calibration points. This is taken as a conservative estimate of the accuracy. There is no evidence of sensor drift.

## 5. Summary

The realtime oxygen data from float 92 Aanderaa optode should be multiplied by 1.034 to achieve calibration accuracy of  $\pm 2 \mu\text{mol/kg}$  within the mixed layer and during the isopycnal drifts. Data from the profiles contains additional errors due to sensor time response that is not corrected. **The Aanderaa optode is the preferred oxygen dataset for analysis.** The Seabird optode has similar accuracy, but is sampled less frequently and has some bad data points.

The oxygen data release contains the adjusted Aanderaa data:

*EXPORTS\_EXPORTSNP\_oxygen\_Aanderaa\_float\_20180814\_R1.sb*

Variables are

date,time	yyyymmdd HH:MM:SS
lat,lon	Position from float GPS interpolated
pressure	Float CTD pressure (positive only), dbar
sample	Pressure including negative values
sal,wt	salinity and temperature, PSU and C
it	Temperature measured by optode, C
amplitude_1id	Red amplitude
amplitude_2id	Blue amplitude
phase	Optode phase, degrees
oxygen_saturation	Realtime oxygen saturation output by optode. %
oxygen_kg	Oxygen concentration from saturation and CTD $\mu\text{mol/kg}$
oxygen_kg_1id	Oxygen concentration calibrated, $\mu\text{mol/kg}$ <b>(USE THIS)</b>

The Seabird optode data is released as

*EXPORTSEXPORSTNP\_oxygen\_Seabird\_float\_20180814\_R1.sb*

Variables are

date,time	yyyymmdd HH:MM:SS
lat,lon	Position from float GPS interpolated
pressure	Float CTD pressure (positive only), dbar
sample	Pressure including negative values
sal,wt	salinity and temperature, PSU and C
it	Temperature measured by optode, C
phase	Optode phase, degrees
oxygen	Realtime oxygen output by optode ml/L
oxygen_kg	Oxygen concentration calibrated, $\mu\text{mol/kg}$

## References

Bittig, H.C., Körtzinger, A., Neill, C., van Ooijen, E., Plant, J.N., Hahn, J., Johnson, K.S., Yang, B. and Emerson, S.R., 2018. Oxygen optode sensors: Principle, characterization, calibration, and application in the ocean. *Frontiers in Marine Science*, 4, p.429.

Bittig, H.C. and Körtzinger, A., 2015. Tackling oxygen optode drift: Near-surface and in-air oxygen optode measurements on a float provide an accurate in situ reference. *Journal of Atmospheric and Oceanic Technology*, 32(8), pp.1536-1543.

T.P. Boyer, J.I. Antonov, H.E. Garcia, D.R. Johnson, R.A. Locarnini, A.V. Mishonov, M.T. Pitcher, O.K. Baranova, I.V. Smolyar, 2006. World Ocean Database 2005. S. Levitus, Ed., NOAA Atlas NESDIS 60, U.S. Government Printing Office, Washington, D.C., 190 pp., DVDs.

Bushinsky, S.M., Emerson, S.R., Riser, S.C. and Swift, D.D., 2016. Accurate oxygen measurements on modified Argo floats using in situ air calibrations. *Limnology and Oceanography: Methods*, 14(8), pp.491-505.

Johnson, K.S., Plant, J.N., Riser, S.C. and Gilbert, D., 2015. Air oxygen calibration of oxygen optodes on a profiling float array. *Journal of Atmospheric and Oceanic Technology*, 32(11), pp.2160-2172.

Nayar, K.G., Sharqawy, M.H. and Banchik, L.D., 2016. Thermophysical properties of seawater: a review and new correlations that include pressure dependence. *Desalination*, 390, pp.1-24.